



Article

# Performances Recovery of Flax Fiber Reinforced Composites after Salt-Fog Aging Test

Luigi Calabrese <sup>1,\*</sup>, Vincenzo Fiore <sup>2</sup>, Riccardo Miranda <sup>2</sup>, Dionisio Badagliacco <sup>2</sup>, Carmelo Sanfilippo <sup>2</sup>, Davide Palamara <sup>1</sup>, Antonino Valenza <sup>2</sup> and Edoardo Proverbio <sup>1</sup>

<sup>1</sup> Department of Engineering, University of Messina, Contrada Di Dio (Sant'Agata), 98166 Messina, Italy

<sup>2</sup> Department of Engineering, University of Palermo, Viale delle Scienze, Edificio 6, 90128 Palermo, Italy

\* Correspondence: lcalabrese@unime.it; Tel.: +39-0906765544

**Abstract:** In the present paper, the performance recovery under conditions of discontinuous exposure to a marine environment of a natural fiber-reinforced composite (NFRC) reinforced by flax fibers was assessed. In particular, this laminate was initially exposed to salt-fog for 15 and 30 days, and then stored in a controlled air condition for up to 21 days. The flax fiber-reinforced composite showed coupled reversible and irreversible aging phenomena during the wet stage, as well as evidencing a significant mechanical recovery during the dry stage. Unlike the stiffness, the laminate showed a noticeable recovery of its flexural strength. This behavior affected the composite material toughness. A simplified approach was applied to define a topological map of the material toughness at varying drying times. The results highlight that the composite shows maximum toughness at intermediate drying times thanks to the strength recovery, in addition to its residual plasticity. This approach allows us to better determine that the strength is more closely related to reversible degradation phenomena, whereas the stiffness is mainly correlated to irreversible ones, implying relevant effects on the toughness of the composite exposed to a wet/dry cycle.

**Keywords:** polymer–matrix composites (PMCs); environmental degradation; natural fibers; wet–dry; aging



**Citation:** Calabrese, L.; Fiore, V.; Miranda, R.; Badagliacco, D.; Sanfilippo, C.; Palamara, D.; Valenza, A.; Proverbio, E. Performances Recovery of Flax Fiber Reinforced Composites after Salt-Fog Aging Test. *J. Compos. Sci.* **2022**, *6*, 264. <https://doi.org/10.3390/jcs6090264>

Academic Editors: Virupaxi Auradi and Deesy G. Pinto

Received: 27 July 2022

Accepted: 7 September 2022

Published: 9 September 2022

**Publisher's Note:** MDPI stays neutral with regard to jurisdictional claims in published maps and institutional affiliations.



**Copyright:** © 2022 by the authors. Licensee MDPI, Basel, Switzerland. This article is an open access article distributed under the terms and conditions of the Creative Commons Attribution (CC BY) license (<https://creativecommons.org/licenses/by/4.0/>).

## 1. Introduction

In recent years, increasing attention has been paid to natural fiber-reinforced composites (NFRCs) due to their peculiar features, such as large availability, low cost, recyclability and eco-friendliness for a sustainable engineering composite design [1]. In the context of natural or vegetable fibers, flax fiber has acquired extensive applicability as a semi-structural and functional reinforcement for composite materials. This success is mainly due to its specific mechanical properties, comparable to those of glass fibers [2].

However, some limiting factors, such as lower and highly variable mechanical properties as well as poor resistance to aging when subjected to humid environmental conditions compared to synthetic fibers, hinder their broader and more consolidated implementation in advanced composite materials fields [3,4].

Natural fibers show an intrinsic hydrophilic nature, owing to the presence of polysaccharide components (i.e., mainly pectin, cellulose and hemicellulose) with strongly polarized hydroxyl groups, which impart a natural predisposition to absorb high quantities of water or humidity [5]. This means that, when exposed to wet environments, natural fibers rapidly undergo a decline in their mechanical performances [6]. At the same time, the weakening of the fiber–matrix interface also leads to a significant decreasing of the adhesive properties, further negatively affecting the responses of the NFRCs in wet or humid environments [7].

The durability of natural fiber-reinforced composites after continuous exposure to humid or wet environments, or after wet/dry aging cycles, has been the subject of sev-

eral research campaigns in the last decade, referring to static mechanical [8,9], dynamic mechanical [10,11], fatigue [12] impact [13] and fracture toughness tests [14].

Furthermore, some research activities specifically evaluated the effects of a wet/dry cyclic aging on the mechanical performances of natural fiber composites [15,16], evidencing noticeable decrements in both strength and stiffness.

Nevertheless, to the best of our knowledge, a very limited range of literature has concerned the evaluation of the ability of these materials to recover their performances under discontinuous exposure to aggressive conditions to date [17,18].

In such a context, the aim of this paper is to assess the performance recovery of flax fiber-reinforced composites under conditions of discontinuous exposure to a marine environment. To this end, flax-reinforced epoxy composites were exposed to a wet/dry aging cycle, which involves the following stages: (i) exposition to salt-fog at 35 °C for 15 and 30 days, (ii) storage in controlled conditions at 50% R.H. and 22 °C between 0 and 21 days. Water sorption analysis and three-point flexural tests were carried out in order to assess reversible and irreversible aging phenomena triggered during the aging treatment. The main goal is addressing the effects of degradation phenomena on the toughness of the composite material at varying drying times, relating this effect to the synergistic action of weakening (influence on strength) and softening (influence of stiffness). For this purpose, a simplified topological representation of the material toughness was proposed.

## 2. Materials and Methods

A twill weave woven flax fabric with nominal areal weight 318 g/m<sup>2</sup> (Lineo, Saint Martin du Tilleul, France) was used as reinforcement for the composite panels.

Flax composite panels were manufactured through vacuum infusion using a two-stage vacuum pump model VE 235 D (Eurovacuum, Reeuwijk, The Netherlands) in order to create maximum vacuum equal to 0.1 atm (absolute). In particular, the cure cycle consisted of a first step at 25 °C for 24 h, followed by a heating at 50 °C for 15 h, according to the technical datasheet of the DEGBA epoxy matrix SX8 EVO (Mates Italiana s.r.l., Milan, Italy). The investigated laminates have stacking sequence [F<sub>5</sub>] and thickness 3.35 ± 0.02 mm.

Following the ASTM B 117 standard [19], the composite material was initially exposed to salt-fog in a climatic chamber model SC/KWT 450 (Weiss, Buchen, Germany) for 15 or 30 days, respectively. In particular, during this stage (defined as wet stage), the temperature inside the chamber was set at 35 ± 1 °C and the chamber reservoir was filled with a 5 wt. % NaCl aqueous solution. Afterwards, prismatic samples to be used for mechanical characterization were cut from the panel with a diamond blade saw and stored at 22 ± 1 °C and 50% R.H., for an interval time of up to 21 days (i.e., dry stage). In particular, five prismatic samples (13 × 64 × 3.35 mm<sup>3</sup>) for each investigated dry time were tested with a three-point bending configuration under displacement control. In more detail, the mechanical tests were carried out in accordance with the ASTM D790 standard, using a Universal Testing Machine (U.T.M.) model Z005 (Zwick-Roell, Ulm, Germany), equipped with 5 kN load cell. The displacement rate and support span were set equal to 1.4 mm/min and 54 mm, respectively. Five replicas for each batch were carried out.

As a function of exposure to the salt spray fog chamber and drying times, all batches were identified with an “FWt1Dt2” code, where t1 and t2 are the time intervals in days of the two stages (i.e., wet and dry), respectively. E.g., FW15D3 indicates samples were exposed to salt-fog and then dried for 15 and 3 days, respectively. Analogously, FW0D0 refers to unaged samples.

With the purpose of analyzing the water uptake evolution with increasing exposure time to the salt-fog environment, according to the ASTM D570 standard, three square samples (100 mm × 100 mm) were removed at specific time intervals from the climatic chamber within the range 1–30 days, cleaned with a dry fabric cloth, and immediately

weighed with the aid of an analytical balance (model AX 224 by Sartorius, Goettingen, Germany). The water uptake  $WU$  of the laminate was calculated as in the following:

$$WU(\%) = \frac{W_t - W_0}{W_0} \cdot 100 \quad (1)$$

where  $W_0$  is the weight of the unaged sample, whereas  $W_t$  is the weight of the sample aged at  $t$  exposure time in a salt-fog environment.

Based on the  $WU$  trend at varying times, we also evaluated the water diffusion coefficient  $D$  of the laminate, both in the absorption and the desorption stage. In particular,  $D$  was calculated as the slope of the  $WU$  versus the square root of the time curve, according to the following equation:

$$D = \pi \left( \frac{h}{4WU_\infty} \right)^2 \left( \frac{WU_2 - WU_1}{\sqrt{t_2} - \sqrt{t_1}} \right)^2 \quad (2)$$

where  $WU_\infty$  is the water uptake at saturation,  $h$  is the thickness of the sample (expressed in mm), and  $(WU_2 - WU_1)/(\sqrt{t_2} - \sqrt{t_1})$  is the slope of the curve in the time interval  $(t_2 - t_1)$ , expressed in s.

Once the wet stage had been completed, the weights of the FW15 and FW30 batches (i.e., exposed to salt-fog for 15 and 30 days, respectively) were periodically acquired during the dry stage in order to assess the mass recovery evolution of the natural fiber-reinforced composite with increasing drying times.

### 3. Results and Discussion

#### 3.1. Water Uptake

Figure 1 shows the trend of water uptake at varying wet and dry times for FW15 and FW30 batches. In particular, the dark and white filled markers refer to samples exposed for 15 days and 30 days to salt-fog (i.e., FW15 and FW30 batches, respectively). It is worth noting that all curves exhibit two different stages:

- At first, during the wet stage, a gradual increase in the water uptake occurred, related to the direct proportionality between wetting time and absorbed water. For long exposure times (see the water uptake trend for the FW30 batch), a slight deviation from this linearity can be noticed. In particular, the maximum water uptake was 7.86% and 10.54% for the FW15 and FW30 batches, respectively. In fact, the curves do not show the clear stabilization of the weight increase, even for long exposure times in a salt spray chamber. This implies that, due to the inherently hydrophilic property of the fiber, the material has not completed its absorption process. Consequently, the natural fiber-reinforced laminate is still potentially sensitive to diffusion phenomena of water molecules. This expected finding can be related to the dramatic tendency to absorb water shown by NFRC materials [19,20];
- At the wet/dry stage transition, the trend in the water uptake curve exhibits an evident inversion point. In particular, the curves' slope for both the investigated batches shows a clear weight reduction (i.e., related to a significant water uptake decrease) after a few days. In particular, the FW15 and FW30 batches exhibited water uptake reductions of 2.92% and 4.52% in the first 24 h of drying, respectively. A stabilization of the weight at an asymptotic constant value was only observed at long drying times. In particular, the batch FW30 showed residual water uptake of about 0.6% higher than that exposed for a shorter time to salt-fog (i.e.,  $M_t \sim 1.86\%$  and  $\sim 2.46\%$  for FW15 and FW30 batches, respectively). This can be considered as quite predictable, because it is widely known that the weight gain of NFRCs exposed to humid or wet environmental conditions or immersed in aqueous solutions is strictly related to the immersion time [21,22].

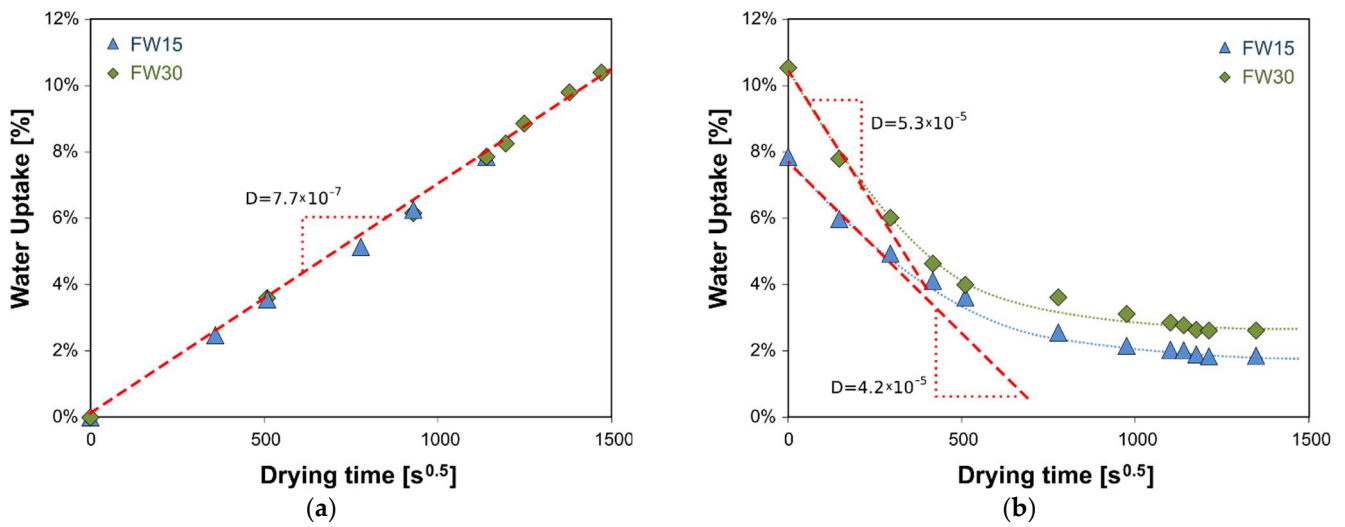


**Figure 1.** Water uptake evolution with increasing time during (a) wet and (b) dry stages for flax laminates. Red lines refer to curved slope.

The initial  $\Delta Mt/\Delta t$  slope, calculated according to Equation (2), can be used to determine the water diffusion coefficients during the adsorption and desorption stages. In particular, the water diffusion coefficient during the wet stage is equal to  $7.7 \times 10^{-7} \text{ mm}^2/\text{s}$  ( $R^2$  equal to 0.99). This value is about two orders of magnitude lower than that related to the desorption one (i.e., dry branch of the curve). In more detail, the FW15 and FW30 batches exhibited desorption diffusion coefficients equal to  $4.2 \times 10^{-5} \text{ mm}^2/\text{s}$  ( $R^2$  equal to 0.95) and  $5.3 \times 10^{-5} \text{ mm}^2/\text{s}$  ( $R^2$  equal to 0.98), respectively. The significant difference between the absorption and desorption phases leads us to infer that, from the kinetic point of view, water absorption can be considered as the limiting factor in the water uptake process during the wet/dry cycle.

### 3.2. Quasi-Static Mechanical Tests

With the intention, as referenced, to outline the mechanical behavior of the NFRC laminate, the evolution of the flexural stress and tangent modulus versus strain for unaged samples are reported in Figure 2a.

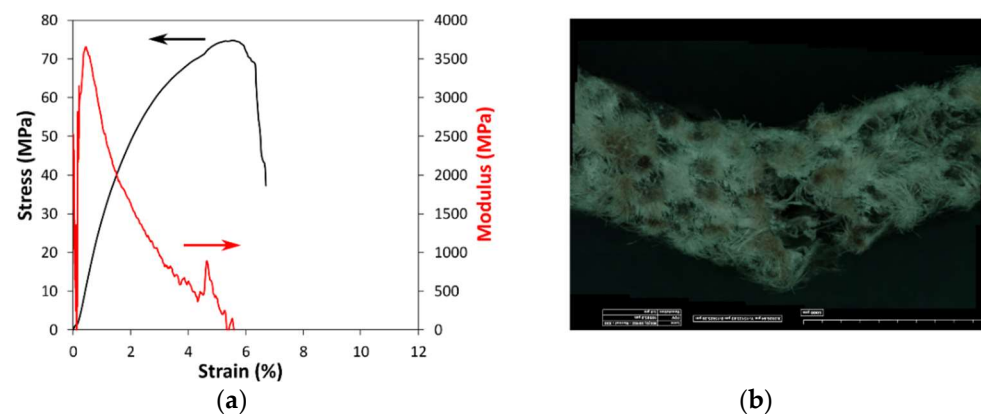


**Figure 2.** (a) Stress and modulus vs. strain plot and (b) related 3D optical image of the flexural fracture surfaces of unaged NFRC (i.e., FW0D0 samples).

Due to the presence of natural fibers, the composite laminate does not show an exclusive elastic behavior [23]. With increasing deflection, there is a progressive deviation from linearity in the stress vs. strain curve. This is confirmed by the elastic modulus trend, which shows a maximum equal to about 3600 MPa at ~0.5% of strain. Once it has exceeded this value, a progressive reduction in the tangent elastic modulus occurs, which indicates

a slight elastoplastic behavior of the material followed by a sudden load drop due to the catastrophic fracturing of the sample.

These considerations are confirmed by observing the 3D optical image of the fractured surface (Figure 2b). An abrupt fracture related to the crack activation and propagation from the external bottom side of the sample (where the maximum tensile stress is reached) evolves transversally to the sample length toward its neutral axis. It is worth noting that the fractured sample does not exhibit evident delamination or secondary crack propagation phenomena.

With the purpose of assessing the mechanical performances decay and recovery induced by the exposure to wet and dry stages, Figure 3 compares the flexural stress and tangent modulus for FW15 and FW30 composite batches at increasing drying times.

By observing Figure 3a, concerning the FW15D0 and FW30D0 samples, it is possible to notice that the water absorbed during the exposition in the saturated moisture environment present in the climatic chamber has a sharp effect on the mechanical performances of the composites, causing great changes in the laminate strength and stiffness. Indeed, the FW15D0 and FW30D0 laminates evidence a significant decrease both in flexural strength and stiffness. The performance decay in the NFRC can be ascribed to the concomitant activation of different degradative phenomena, triggered during the aging cycle, that play a synergistic role in the worsening of the composite performances.

In particular, water absorption leads to the swelling of the composite constituents, thus triggering micro-cracking [15], softening and plasticization [24]. This induces a decrease in the crack activation and propagation stress limit in the composite laminate [25].

Furthermore, the stress–strain curve and the related tangent modulus trend clearly evidence that a transition from mainly linear to nonlinear mode occurs. Furthermore, the fracture mode evolves from catastrophic to progressive at increasing aging times in the salt-fog environment. The high strain at failure reached suggests a ductile failure mode stimulated by relevant interlaminar and in-plane shear stresses able to generate delamination and shear degradation phenomena [26]. The flexural fracture image of the FW30D0 samples did not exhibit a clear mechanical collapse in the span centerline. This sample experienced a noticeable deflection, without showing critical failure cracks due to the ductile behavior of the wet aged flax and matrix constituents [27].

The dry stage facilitates in the composite laminate the gradual recovery of its mechanical performances (Figure 3b,c). In particular, progressive improvements in the maximum flexural strength and elastic modulus occur at increasing drying times. At the same time, the strain at failure exhibits a gradual decrease. This indicates that some of the degradative phenomena, already activated during the wet stage (such as plasticization or softening), reversibly affect the mechanical performances of the NFRC. In particular, the composite laminate showed the recovery of its initial maximum flexural strength after a long drying time (see Figure 3c). Moreover, the strain at failure of FW15D21 samples is about twice that of FW0D0 samples. Similarly, the FW30D21 samples show maximum strength and stiffness values of about 7% and 27% lower than that of the unaged samples (i.e., FW0D0).

These findings are confirmed by evaluating the 3D optical image of the flexural fractures of FW30D3 and FW30D21 samples. The failure is triggered by the tensile crack activation of the external bottom laminae. Then, this progressively evolves, growing toward the laminate neutral axis, thus activating secondary failure mechanisms such as debonding, pull-out or interlaminar shear fracture.

The water absorbed during the wet stage activates simultaneous degradative phenomena, which have different effects on the mechanical stability of the material. Furthermore, these mechanisms offer different reversible and irreversible contributions that can influence the residual mechanical properties of the composite at the end of the dry stage. Remarkably, the NFRC still retains high ductility at the end of the dry stage, meaning that the laminate has a partially compromised stiffness. On the contrary, the maximum flexural stress can be considered mainly recovered: i.e., the stress reduction undergone during the wet stage can

be correlated to reversible degradative phenomena. On the contrary, the stiffness decay can be more likely ascribed to coupled reversible and irreversible aging phenomena.

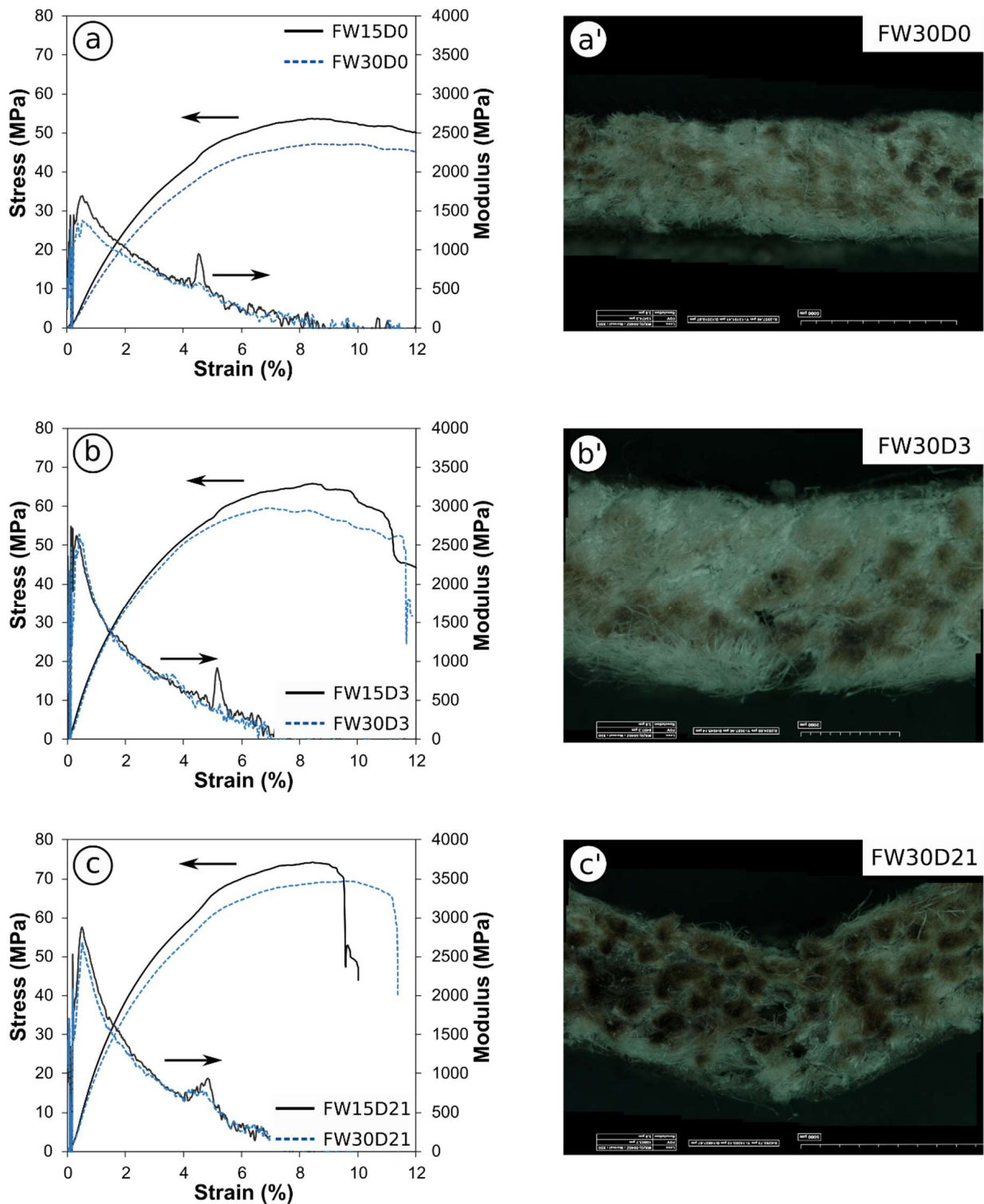


Figure 3. Stress and modulus vs. strain plot at varying wet–dry times for flax laminates: (a,a') 0 days; (b,b') 3 days; (c,c') 21 days of dry time.

The experimental results of the mechanical tests are listed in Table 1, which reports the average values and the related standard deviations of the flexural performance parameters (i.e., maximum stress  $\sigma$ , elastic modulus  $E$  and strain at the maximum stress  $\epsilon_{peak}$ ) at varying wet–dry times.

The experimental results clearly show the already discussed effects of wet and dry stages on the quasi-static flexural properties of the composite. In particular, the exposure to salt-fog leads to a reduction in both maximum strength (i.e., −29% and −31% after 15 and 30 days of exposure, respectively) and flexural modulus (i.e., −31% and −50% after 15 and 30 days of exposure, respectively). On the other hand, the strain at break of the laminate increases after the wet stage, reaching 66% higher values in comparison to the unaged laminates, regardless of the exposure time to salt-fog. The followed dry stage allows the recovery of almost all the initial maximum strength (i.e., 73.9 MPa and 72.7 MPa for FW15D21 and FW30D21 samples versus 74.5 MPa for unaged FW0D0 samples), whereas the flexural modulus recovery was found to be only partial (i.e., 3.0 GPa and 2.7 GPa for FW15D21 and FW30D21 samples versus 3.4 GPa for unaged FW0D0 samples).

**Table 1.** Main flexural properties at varying wet–dry times for flax laminates.

	$\sigma$ (MPa)		E (GPa)		$\epsilon_{peak}$ (%)	
	Avg	Std.dev.	Avg	Std.dev.	Avg	Std.dev.
FW0D0	74.5	4.4	3.4	0.2	5.3	0.2
FW15D0	53.2	0.9	1.9	0.0	8.8	0.4
FW15D0.25	57.3	6.4	2.3	0.2	8.9	0.2
FW15D1	61.0	2.3	2.3	0.1	8.8	0.4
FW15D2	66.3	4.6	2.6	0.2	8.8	0.4
FW15D3	66.7	2.2	2.9	0.0	8.6	0.6
FW15D7	67.5	4.4	2.7	0.3	8.2	0.4
FW15D11	72.6	3.5	2.9	0.2	8.4	0.6
FW15D21	73.9	3.9	3.0	0.2	8.0	0.7
FW30D0	51.1	2.8	1.7	0.3	8.8	0.4
FW30D0.25	54.8	0.8	1.8	0.2	8.8	0.6
FW30D1	54.7	1.2	1.9	0.2	9.1	0.7
FW30D2	64.4	5.7	2.4	0.3	9.2	0.8
FW30D3	63.9	3.3	2.5	0.4	9.0	1.0
FW30D7	67.6	4.1	2.7	0.4	9.2	0.7
FW30D11	67.9	1.3	2.7	0.2	9.1	0.8
FW30D21	72.7	2.2	2.7	0.2	9.0	0.7

In order to better understand how the mechanical properties are reduced due to the aging during salt-fog exposure, and their eventual recovery after the drying cycle, it may be useful to define the dimensional indices relating to the decay/recovery of the strength and stiffness of the composite laminate. In particular, a flexural strength ratio (FSR) and elastic modulus ratio (EMR) can be defined as in the following:

$$FSR = \frac{E_{Dry\_t}}{E_0} \tag{3}$$

$$FMR = \frac{\sigma_{Dry\_t}}{\sigma_0} \tag{4}$$

where  $E_{Dry\_t}$  and  $\sigma_{Dry\_t}$  are the flexural elastic modulus and strength values of the laminate after at “ $t$ ” drying time. Analogously,  $E_0$  and  $\sigma_0$  are the flexural elastic modulus and strength values of the unaged laminate, respectively. These indices are correlated to the percentage of recovery of the performance of the unaged composite. For instance, an FSR index equal to 0.8 indicates that the material has a flexural strength equal to 80% of the unaged material. Consequently, the same index value also provides indirect information concerning a residual decay of 20% (i.e., 1.0–0.8) of the mechanical strength. Similar considerations can be drawn concerning the FMR index related to the stiffness of the composite.

In this context, Figure 4 shows the evolution of FMR vs. FSR indices at varying drying times, both for FW15 and FW30 batches.

It is possible to notice that longer exposure in the climatic chamber (batch FW30Dx compared to FW15Dx) leads to a decrease in both FSR and FMR indices. In particular, the

FW30Dx curve is slightly shifted to the left, compared to the FW15Dx one, meaning that the composite laminate is unable to effectively recover the initial stiffness. These results indicate that the elastic modulus is sensitive to permanent degradative phenomena, which take place and contribute more significantly with a greater the wet stage.

The last considerations cannot be made for the FSR index. Although at short drying times, the FW30DX batch shows lower FSR indices, the difference between the compared batches becomes progressively less relevant at increasing drying times. As already stated, these results show that the degradative phenomena occurring during the wet stage induce decays in both strength and stiffness performances. However, the mechanisms responsible for the flexural strength decay are mainly reversible, leading to comparable strength values between FW15Dx and FW30Dx batches at the end of the dry stage.

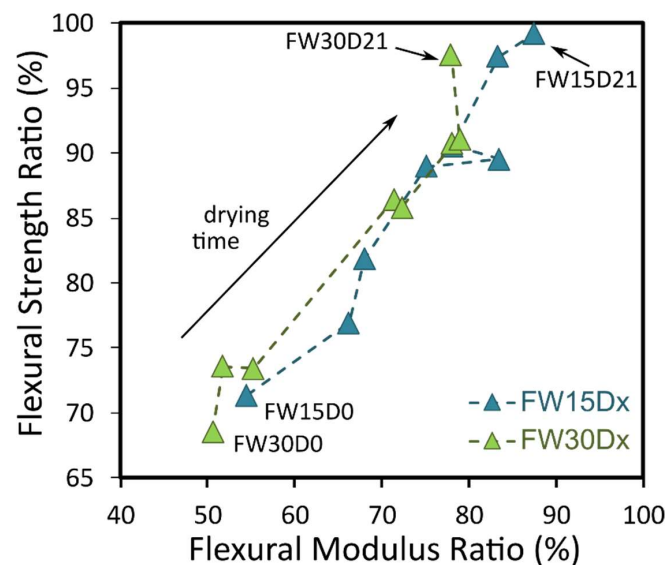


**Figure 4.** Flexural strength vs. modulus ratio at varying dry times of flax laminates.

These findings indicate that the natural fiber-reinforced composite shows irreversible softening degradative phenomena, which affect its strength and stiffness in different ways [28].

### 3.3. Toughness Map

To understand better how this plays a role in the mechanical stability of the laminate, an approach aimed at evaluating the evolution of the laminate's toughness under varying wet and dry conditions may be useful. This can indicate the energy required by the natural fiber composite laminate for breaking. As is widely known, the toughness (i.e., the amount of energy that the natural fiber composite laminate can absorb to reach its breaking condition) is proportional to the area under the flexural stress–strain curve [29,30]. Hence, tough materials are always characterized by high strength and/or strain at break values.

In such a context, some fundamental parameters have been identified in the typical stress–strain curve shown in Figure 5. In particular, the area under the curve can be seen roughly as a trapezoid, whose height can be considered equal to the maximum stress value. The major base can be represented by the strain at break value. Finally, a further parameter,  $\epsilon_{\sigma_{\max}}$ , defined as the difference between strain values identified on the curve in correspondence to 90% of the maximum stress, can be identified as the minor base of the trapezoid.

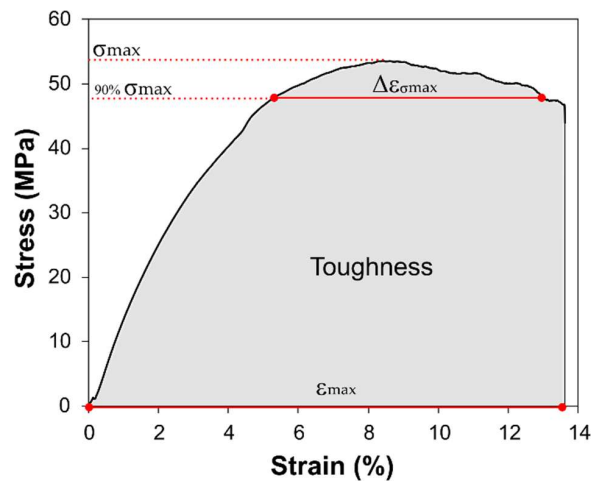


Figure 5. Main stress–strain parameters for toughness evaluation.

Based on this approach, Figure 6 can be identified as a topological representation of the material toughness. The graph has “ $\epsilon_{\max} + \epsilon_{\sigma_{\max}}$ ” as the x axis and “ $\sigma_{\max}$ ” as the y axis. This plot can be used to assess the variation in strength and ductility of the composite material, allowing us also to correlate this indirectly to the toughness characteristics of the composite laminate. In particular, the red dotted lines are iso-toughness curves (calculating the area of the trapezoid geometry, considering the x-axis is the sum of minor and major bases and the y-axis is the height of the trapezoid), which discretize the plot into three regions: i.e., low, medium and high toughness.

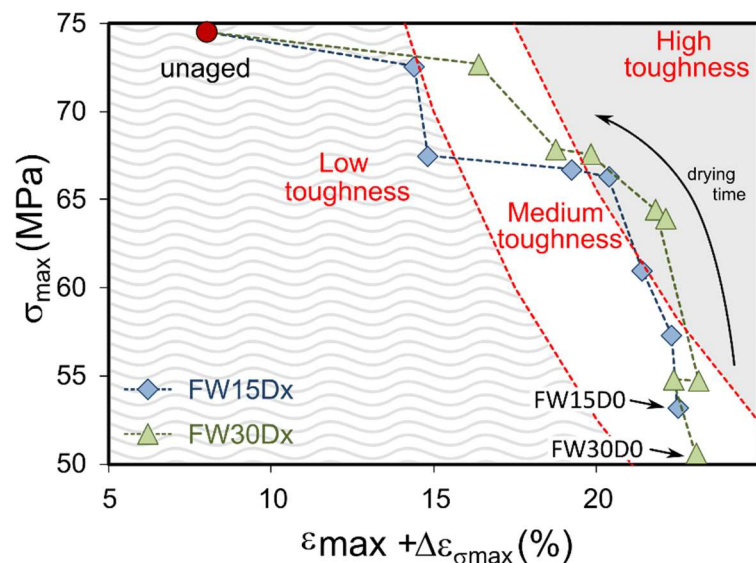


Figure 6.  $\sigma_{\max}$  vs.  $\epsilon_{\max} + \epsilon_{\sigma_{\max}}$  plots for FW15 and FW30 samples.

This graph shows that the unaged sample exhibits brittle behavior with a high maximum stress and low deformation at break, thus leading to low toughness. The exposure to salt-fog induces a toughness enhancement due to a significant increase in  $\epsilon_{\max} + \epsilon_{\sigma_{\max}}$ , which compensates for the maximum stress reduction due to the weakening phenomena occurring during the wet stage.

By analyzing the behavior of the wet samples (i.e., not dried), no significant difference can be observable between FW15D0 and FW30D0 batches (see points in the lower right corner of the figure). The exposure for 30 days to salt-fog leads to the activation of softening and weakening phenomena. The area under the stress–strain curve is not significantly affected, though, inducing a toughness of the material comparable between FW15 and FW30 batches.

Interesting considerations can be drawn by evaluating the evolution of the curves as the drying time varies. By increasing the drying time, the samples show a progressive increase both in stiffness and strength, as previously highlighted.

This results in the increase in the mechanical parameters linked to stress (i.e.,  $y$ -axis in Figure 6) and to deformation (i.e.,  $x$ -axis). However, the FW30 batch shows a residual deformation at break, which cannot be recovered during the dry stage (i.e., the FW30 curve in Figure 6 is shifted to the right compared to the FW15 one). The consequence is the presence of greater softening on the composite laminate, which enhances the toughness of the FW30 batch. A similar behavior, although less evident, was also observed for the FW15 batch. Indeed, both laminates shifted from the medium-toughness region to the high-toughness one with an increasing drying time. This finding is the consequence of an increase in the area under the stress–strain curve, which, as evidenced by Figure 6, is due to a significant increase in the  $\sigma_{\max}$ , as well as to the limited reduction in  $\epsilon_{\max} + \epsilon_{\sigma_{\max}}$  parameter.

After completing the 21-day dry stage, the FW30D21 samples exhibited a quite similar maximum stress value in comparison to the FW15D21 ones. However, their higher  $\epsilon_{\max} + \epsilon_{\sigma_{\max}}$  parameter led to higher residual toughness for the batch exposed longer to the salt-fog.

These results highlight the relevant correlation between the environmental conditions and the mechanical behavior of the natural fiber-reinforced composite. In more detail, the toughness of the NFRC laminate, influenced by softening and weakening phenomena, is particularly sensitive to wet-dry stages, exhibiting a progressive transition from low to high values. Future investigations will aim to better discriminate the effects of reversible and irreversible mechanisms on the material toughness, as well as to define strategies (e.g., hybridization with synthetic fibers) to improve mechanical stability in severe wet environments, thus enhancing the knowledge in this research context.

#### 4. Conclusions

In order to clarify the effect of the aging cycles on the mechanical performances, flax-reinforced epoxy composite samples were exposed to a wet/dry cycle, and their water sorption and flexural properties were monitored at varying times of wet and dry stages. By way of summarizing, it can be concluded that:

- The degradation mechanisms that take place during the wet stage affect both the strength and stiffness of flax fiber-reinforced composites in different ways. In particular, after 30 days of salt-fog exposure, FW30 laminates showed decays in strength and stiffness of 31% and 49%, respectively;
- The performance reductions are recovered during the dry stage. Unlike stiffness, the composite laminate is able to recover almost completely its initial flexural strength. In particular, the FW30D21 batch exhibited recovery values of 98% and 78% in terms of strength and stiffness, respectively.

The different strength and stiffness trends also affect the material toughness, which was found to be highest with intermediate drying times. These findings were summarized in a simplified topological toughness map seeking to highlight visually the toughness performances of the laminate in relation to its maximum resistance and ductility. Overall, the toughness of the natural fiber-reinforced laminate, being affected by softening and weakening phenomena, is noticeably influenced by its exposure to a wet–dry environment, exhibiting a progressive transition from low to high values.

**Author Contributions:** Conceptualization, L.C.; methodology, L.C. and V.F.; validation, V.F.; formal analysis, L.C. and V.F.; investigation, R.M., D.B., C.S. and D.P.; data curation, D.P., L.C. and V.F.; writing—original draft preparation, L.C.; writing—review and editing, V.F.; supervision, project administration, funding acquisition, A.V. and E.P. All authors have read and agreed to the published version of the manuscript.

**Funding:** This research was funded by “SI-MARE—Soluzioni Innovative per Mezzi navali ad Alto Risparmio Energetico” (P.O. FESR Sicilia 2014/2020, grant number 08ME7219090182) founded by Regione Sicilia.

**Data Availability Statement:** The data presented in this study are available on request from the corresponding author.

**Conflicts of Interest:** The authors declare no conflict of interest.

## References

1. Yan, L.; Chouw, N.; Jayaraman, K. Flax fibre and its composites—A review. *Compos. Part B Eng.* **2014**, *56*, 296–317. [[CrossRef](#)]
2. Lotfi, A.; Li, H.; Dao, D.V.; Prusty, G. Natural fiber–reinforced composites: A review on material, manufacturing, and machinability. *J. Thermoplast. Compos. Mater.* **2019**, *34*, 238–284. [[CrossRef](#)]
3. Chandrasekar, M.; Ishak, M.R.; Sapuan, S.M.; Leman, Z.; Jawaid, M. A review on the characterisation of natural fibres and their composites after alkali treatment and water absorption. *Plast. Rubber Compos.* **2017**, *46*, 119–136. [[CrossRef](#)]
4. Azwa, Z.N.; Yousif, B.F.; Manalo, A.C.; Karunasena, W. A review on the degradability of polymeric composites based on natural fibres. *Mater. Des.* **2013**, *47*, 424–442. [[CrossRef](#)]
5. Dhakal, H.N.; Zhang, Z.Y.; Richardson, M.O.W. Effect of water absorption on the mechanical properties of hemp fibre reinforced unsaturated polyester composites. *Compos. Sci. Technol.* **2007**, *67*, 1674–1683. [[CrossRef](#)]
6. Muñoz, E.; García-Manrique, J.A. Water absorption behaviour and its effect on the mechanical properties of flax fibre reinforced bioepoxy composites. *Int. J. Polym. Sci.* **2015**, *2015*, 16–18. [[CrossRef](#)]
7. El Hachem, Z.; Céline, A.; Challita, G.; Branchu, S.; Le Duigou, A.; Fréour, S. Dimensional variation and evolution of mechanical properties of wet aged composites reinforced with flax fibers. *J. Compos. Mater.* **2020**, *55*, 1131–1148. [[CrossRef](#)]
8. Pisupati, A.; Bonnaud, L.; Deléglise-Lagardère, M.; Park, C.H. Influence of Environmental Conditions on the Mechanical Properties of Flax Fiber Reinforced Thermoset Composites. *Appl. Compos. Mater.* **2021**, *28*, 633–649. [[CrossRef](#)]
9. Fiore, V.; Sanfilippo, C.; Calabrese, L. Influence of sodium bicarbonate treatment on the aging resistance of natural fiber reinforced polymer composites under marine environment. *Polym. Test.* **2019**, *80*, 106100. [[CrossRef](#)]
10. Fiore, V.; Sanfilippo, C.; Calabrese, L. Dynamic Mechanical Behavior Analysis of Flax/Jute Fiber-Reinforced Composites under Salt-Fog Spray Environment. *Polymers* **2020**, *12*, 716. [[CrossRef](#)]
11. Fiore, V.; Calabrese, L.; Di Bella, G.; Scalici, T.; Galtieri, G.; Valenza, A.; Proverbio, E. Effects of aging in salt spray conditions on flax and flax/basalt reinforced composites: Wettability and dynamic mechanical properties. *Compos. Part B Eng.* **2016**, *93*, 35–42. [[CrossRef](#)]
12. Mejri, M.; Toubal, L.; Cuillière, J.C.; François, V. Hygrothermal aging effects on mechanical and fatigue behaviors of a short-natural-fiber-reinforced composite. *Int. J. Fatigue* **2018**, *108*, 96–108. [[CrossRef](#)]
13. Fiore, V.; Scalici, T.; Sarasini, F.; Tirilló, J.; Calabrese, L. Salt-fog spray aging of jute-basalt reinforced hybrid structures: Flexural and low velocity impact response. *Compos. Part B Eng.* **2017**, *116*, 99–112. [[CrossRef](#)]
14. Hassan, A.; Khan, R.; Khan, N.; Aamir, M.; Pimenov, D.Y.; Giasin, K. Effect of Seawater Ageing on Fracture Toughness of Stitched Glass Fiber/Epoxy Laminates for Marine Applications. *J. Mar. Sci. Eng.* **2021**, *9*, 196. [[CrossRef](#)]
15. Cadu, T.; Van Schoors, L.; Sicot, O.; Moscardelli, S.; Divet, L.; Fontaine, S. Cyclic hygrothermal ageing of flax fibers’ bundles and unidirectional flax/epoxy composite. Are bio-based reinforced composites so sensitive? *Ind. Crops Prod.* **2019**, *141*, 111730. [[CrossRef](#)]
16. Van Schoors, L.; Cadu, T.; Moscardelli, S.; Divet, L.; Fontaine, S.; Sicot, O. Why cyclic hygrothermal ageing modifies the transverse mechanical properties of a unidirectional epoxy-flax fibres composite? *Ind. Crops Prod.* **2021**, *164*, 113341. [[CrossRef](#)]
17. Ventura, H.; Claramunt, J.; Navarro, A.; Rodriguez-Perez, M.A.; Ardanuy, M. Effects of Wet/Dry-Cycling and Plasma Treatments on the Properties of Flax Nonwovens Intended for Composite Reinforcing. *Materials* **2016**, *9*, 93. [[CrossRef](#)]
18. Calabrese, L.; Fiore, V.; Piperopoulos, E.; Badagliacco, D.; Palamara, D.; Valenza, A.; Proverbio, E. In situ monitoring of moisture uptake of flax fiber reinforced composites under humid/dry conditions. *J. Appl. Polym. Sci.* **2021**, *139*, 51969. [[CrossRef](#)]
19. Le Duigou, A.; Davies, P.; Baley, C. Seawater ageing of flax/poly (lactic acid) biocomposites. *Polym. Degrad. Stab.* **2009**, *94*, 1151–1162. [[CrossRef](#)]
20. Yan, L.; Chouw, N. Effect of water, seawater and alkaline solution ageing on mechanical properties of flax fabric/epoxy composites used for civil engineering applications. *Constr. Build. Mater.* **2015**, *99*, 118–127. [[CrossRef](#)]
21. Zamri, M.H.; Akil, H.M.; Bakar, A.A.; Ishak, Z.A.M.; Cheng, L.W. Effect of water absorption on pultruded jute/glass fiber-reinforced unsaturated polyester hybrid composites. *J. Compos. Mater.* **2011**, *46*, 51–61. [[CrossRef](#)]

22. Hristozov, D.; Wroblewski, L.; Sadeghian, P. Long-term tensile properties of natural fibre-reinforced polymer composites: Comparison of flax and glass fibres. *Compos. Part B Eng.* **2016**, *95*, 82–95. [[CrossRef](#)]
23. Chegiani, F.; El Mansori, M.; Chebbi, A.-A. Cutting behavior of flax fibers as reinforcement of biocomposite structures involving multiscale hygrometric shear. *Compos. Part B Eng.* **2021**, *211*, 108660. [[CrossRef](#)]
24. Stamboulis, A.; Baillie, C.A.; Peijs, T. Effects of environmental conditions on mechanical and physical properties of flax fibers. *Compos. Part A Appl. Sci. Manuf.* **2001**, *32*, 1105–1115. [[CrossRef](#)]
25. Moudood, A.; Rahman, A.; Öchsner, A.; Islam, M.; Francucci, G. Flax fiber and its composites: An overview of water and moisture absorption impact on their performance. *J. Reinf. Plast. Compos.* **2019**, *38*, 323–339. [[CrossRef](#)]
26. Haghghatnia, T.; Abbasian, A.; Morshedian, J. Hemp fiber reinforced thermoplastic polyurethane composite: An investigation in mechanical properties. *Ind. Crops Prod.* **2017**, *108*, 853–863. [[CrossRef](#)]
27. Fiore, V.; Calabrese, L.; Miranda, R.; Badagliacco, D.; Sanfilippo, C.; Palamara, D.; Valenza, A.; Proverbio, E. On the response of flax fiber reinforced composites under salt-fog/dry conditions: Reversible and irreversible performances degradation. *Compos. Part B Eng.* **2022**, *230*, 109535. [[CrossRef](#)]
28. Fiore, V.; Calabrese, L.; Miranda, R.; Badagliacco, D.; Sanfilippo, C.; Palamara, D.; Valenza, A.; Proverbio, E. Assessment of performance degradation of hybrid flax-glass fiber reinforced epoxy composites during a salt spray fog/dry aging cycle. *Compos. Part B Eng.* **2022**, *238*, 109897. [[CrossRef](#)]
29. Sheinbaum, M.; Sheinbaum, L.; Weizman, O.; Dodiuk, H.; Kenig, S. Toughening and enhancing mechanical and thermal properties of adhesives and glass-fiber reinforced epoxy composites by brominated epoxy. *Compos. Part B Eng.* **2019**, *165*, 604–612. [[CrossRef](#)]
30. Javanshour, F.; Prapavesis, A.; Pärnänen, T.; Orell, O.; Belone, M.L.; Layek, R.K.; Kanerva, M.; Kallio, P.; Van Vuure, A.W.; Sarlin, E. Modulating impact resistance of flax epoxy composites with thermoplastic interfacial toughening. *Compos. Part A Appl. Sci. Manuf.* **2021**, *150*, 106628. [[CrossRef](#)]